Indirect Detection of Short-lived Hydride Intermediates of Iridium N-Heterocyclic Carbene Complexes via Chemical Exchange Saturation Transfer (CEST) Spectroscopy

Stephan Knecht[a,b&], Sara Hadjiali,[a&], Danila A. Barskiy[c&], Alexander Pines[c], Grit Sauer[a], Alexey S. Kiryutin[d], Konstantin L. Ivanov[d], Alexandra V. Yurkovskaya[d] and Gerd Buntkowsky[a*]

[a]*Eduard-Zintl Institute for Inorganic and Physical Chemistry, TU Darmstadt, Darmstadt, 64287, Germany*
[b] *Department of Radiology, Medical Center – University of Freiburg, Freiburg, 79106, Germany*
[c]*Department of Chemistry, University of California at Berkeley, CA 94720-3220*
[e] *International Tomography Center, Siberian Branch of the Russian Academy of Science, Novosibirsk, 630090, Russia and Novosibirsk State University, Novosibirsk, 630090, Russia*

Supporting Information Placeholder

ABSTRACT: For the first time chemical-exchange saturation transfer (CEST) ^{1}H NMR is utilized for the study of short-lived hydride intermediates in the catalytic cycle of the Iridium-based organometallic complex $[Ir(IMes)(Py)_3(H)_2]Cl$, which are often not observable by other NMR techniques, since they are low concentrated, and undergo reversible ligand exchange with the main complex. The intermediate complexes $[Ir(Cl)(IMes)(Py)_2(H)_2]$ and $[Ir(CD_3OD)(IMes)(Py)_2(H)_2]$ are detected, assigned and characterized *in situ* and at room temperature in solution. Understanding the effects on the spin dynamics induced by these complexes is necessary for enhancing the performance of the nuclear spin hyperpolarization technique SABRE (Signal Amplification By Reversible Exchange). By eliminating $[Ir(Cl)(IMes)(Py)_2(H)_2]$ and manipulating the spin-system by RF-irradiation, we were able to increase the nuclear spin singlet lifetime of the two protons in the main hydride complex by more than an order of magnitude, from 2.2±0.1 s to 27.2±1.2 s. The presented CEST NMR approach has a large application potential for studying short-lived hydride intermediates in catalytic reactions.

Organometallic complexes are widely used in chemistry, both in academic research and in industry, ranging from hydrogenation and polymerization reactions, to the production of fine chemicals and semiconductors.[1-10] However, characterisation of these complexes and the illumination of their reaction pathways remains challenging.[11-12] This is not surprizing because transformations of organometallic complexes in solution often involve the formation of short-lived reaction intermediates present in low concentrations and, therefore, inaccessible to commonly used detection techniques, such as nuclear magnetic resonance (NMR) spectroscopy. Understanding the structure and dynamics of such intermediates is necessary not only for chemical research and catalysis but also for the improved control of nuclear spin states. For example, hydride complexes of Ir and Rh are often employed in hyperpolarization techniques utilizing parahydrogen, a nuclear spin isomer of the hydrogen molecule with the total nuclear spin of zero. In these hyperpolarization techniques, such as parahydrogen-induced polarization (PHIP)[13-17] and signal amplification by reversible exchange (SABRE),[18-21] the enriched singlet state of parahydrogen is converted into magnetization of a reaction product or exchanging species. This process results in significant (several orders of magnitude) increase in signal-to-noise ratio (SNR) of NMR signals and allows preparing hyperpolarized molecules for a variety of applications.[22-25]

The iridium complex $[Ir(IMes)(H)_2(Py)_3]^+Cl^-$ (**1**) is extensively used for SABRE hyperpolarization.[18-21] Recently, experimental evidence has suggested that the evolution of hydrogen spin states in organometallic complexes is strongly influenced by the formation of short-lived intermediates.[26-28] In particular, it has been suggested that parahydrogen in solution suffers a rapid loss of coherence possibly due to the presence of, until now,

unknown reaction intermediates. Such a loss of coherences (also known as singlet-triplet leakage[29]) is expected to dramatically lower the efficiency of SABRE schemes at high fields.[27, 30] This hypothesis is substantiated by a recent demonstration, that SABRE can be significantly more effective at low magnetic fields,[31] where the singlet-triplet leakage is expected to be substantially reduced.[29]

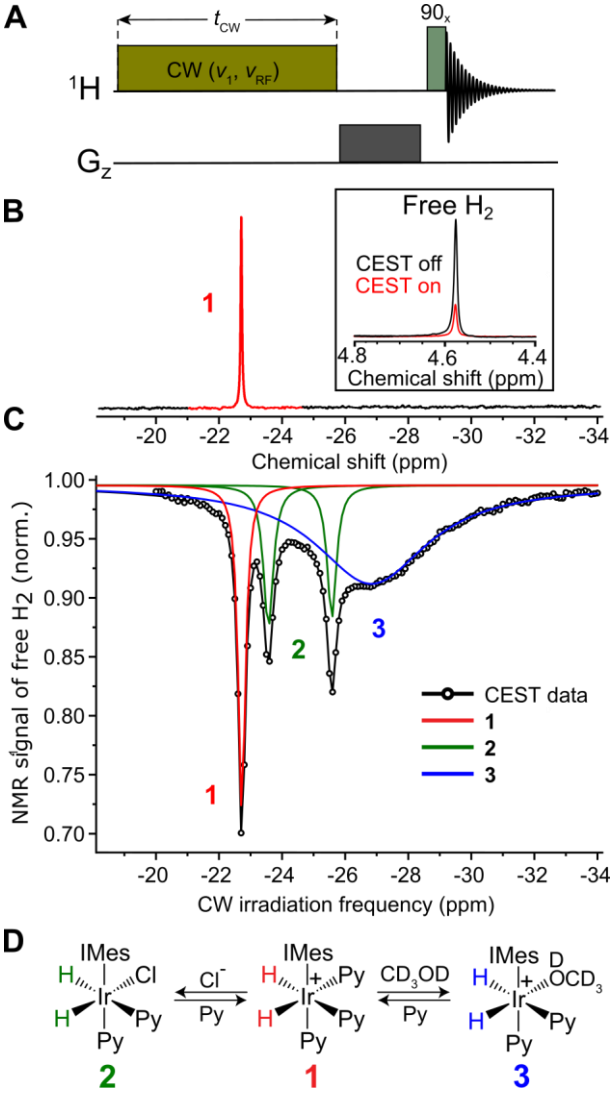

Figure 1: A) Experimental ^{1}H NMR CEST scheme. Continuous wave (CW) irradiation with an amplitude (ν_1 = 50 Hz) is applied for 3 s at a particular offset frequency ν_{RF} and the integral of the free H_2 signal is recorded; then the offset frequency is incremented and the experiment is repeated again yielding the CEST spectrum. B) Standard ^{1}H NMR (500 MHz) spectrum of **1** in methanol-d_4. The inset shows the CEST effect on the free H_2 resonance when saturation is applied to the hydrides of **1** (ν_{RF} = 22.72 ppm). C) ^{1}H NMR CEST spectrum of **1** in methanol at 280 K showing the presence of dihydride intermediates **2** and **3**. Black circles and a black line — experimental data; red, blue and green lines are Lorentzian fits. D) Molecular diagram of the exchange between the main organometallic complex $[Ir(IMes)(H)_2(Py)_3]^+Cl^-$ (**1**) and its intermediates **2** and **3** in solution (methanol-d_4). The exchange with free hydrogen in solution and the direct exchange between **2** and **3** are omitted (see ESI for full scheme).

This is intriguing because only the dihydride **1** is usually observed in conventional as well as in hyperpolarized room-temperature ^{1}H NMR experiments, showing that potential intermediates are too short-lived or present in too low concentration for efficient detection under ambient conditions.[18, 28, 32] Thus the quest is out to experimentally search for such intermediates, which could be present after activation of the catalytic precursor [Ir(IMes)(COD)Cl] (IMes = 1,3-bis(2,4,6-trimethylphenyl)-imidazolium, COD = cyclooctadien) in hydrogen atmosphere and under excess substrate (Py = pyridine). In the present paper, we were interested to explore whether it is possible to reveal and characterize such elusive intermediates at room temperature under ambient conditions, employing indirect detection with the Chemical Exchange Saturation Transfer (CEST)[33-37] experiment.

CEST is a magnetization transfer experiment, where a narrow-band saturation pulse with frequency ν_{RF} is applied, prior to a broad band NMR detection (**Figure 1A**). By varying ν_{RF}, the CEST spectrum is recorded. In our study, we use a continuous wave (CW) saturation pulse, whose effects are detected by virtue of the reduction of the easily-detectable signal of free dissolved H_2, which is reduced by the saturation of exchanging hydrides bound to one of the organometallic complexes (**Figure 1B**). In a previous paper we had described the related PANEL (PArtially NEgative Line)[38] experiment, where the signal of hidden intermediates is indirectly detected via the partially negative hyperpolarized signal of the free hydrogen pool interacting with the complex.

Figure 1 compares the conventional ^{1}H NMR (**Figure 1B**) and the CEST spectrum (**Figure 1C**) of **1** dissolved in methanol-d_4 and pyridine (for experimental details see ESI). While the conventional ^{1}H NMR spectrum exhibits only a single signal at -22.72 ppm, the CEST spectrum consists of four contributions, a strong signal at -22.72 ppm with a signal reduction of 30%, two weaker signals of practically equal intensity at -23.69 and -25.71 ppm with a signal reduction of ca. 15% and a broad signal at –26.71 ppm with a signal reduction of ca. 10%. By virtue of the chemical shift we attribute the strong signal at -22.72 ppm, present in both spectra to the hydrides of species **1**.

The narrow signals at -23.69 and -25.71 ppm in the CEST spectrum indicate the presence of an intermediate with two inequivalent hydrides. In a previous study[32], weak peaks with similar chemical shifts were observed at low temperature and were assigned to the solvent-binding complex $[Ir(IMes)(Py)_2(CD_3OD)(H)_2]^+Cl^-$. A more recent study[39], however, reported similar chemical shift values (-22.77 ppm and −23.78 ppm) for the complex

$[IrCl(H)_2(IMes)(Qu)_2]$ (Qu = quinazoline) in dichloromethane, suggesting that these signals belong to complex $[Ir(Cl)(IMes)(Py)_2(H)_2]$ (**2**).

To conclusively probe the assignment**,** experiments in neat pyridine-d_5 were performed (no CD_3OD was present in the sample). In this case both **1** and **2** are directly observable, with **2** being the dominant form (**Figure 2C)**). However, **2** can be readily removed from solution by exchanging Cl^- with PF_6^-, leaving **1** as the only detectable species (**Figure 2B**). When $[Ir(PCy_3)(COD)(Py)]^+PF_6^-$ (Crabtree's catalyst) was exposed to H_2 in neat pyridine-d_5, only a single species $[Ir(PCy_3)(H)_2(Py)_3]^+PF_6^-$ (**1'**) is observed, (**Figure 2D**). However, after addition of DCl to the sample two hydride peaks of $[Ir(Cl)(PCy_3)(H)_2(Py)_2]$ (**2'**) manifest themselves in the spectrum (**Figure 2E**). As a final proof for the reversible chlorine exchange, we performed a CEST experiment on a sample of **1** in methanol-d_4 after ion-exchange of Cl^- with PF_6^- (see Figure S1, ESI). The disappearance of the doublet lines of **2** from the CEST data confirmed the elimination of **2** from the system and thus proves the assignment of **2** to $[Ir(Cl)(IMes)(Py)_2(H)_2]$.

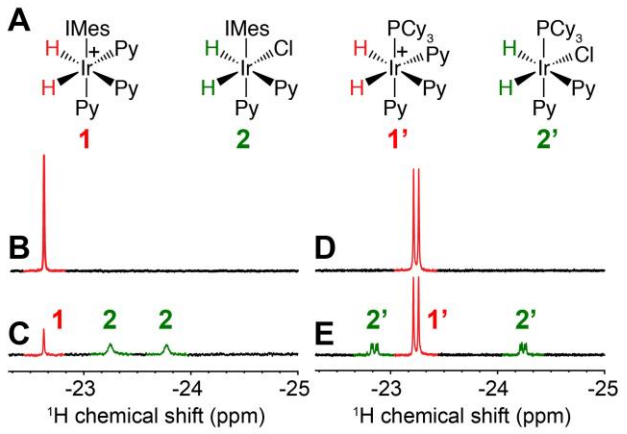

Figure 2: A) Chemical structure of different hydride species (**1**, **2**, **1'**, **2'**) observed by ^1H NMR when [Ir(IMes)(COD)Cl] and $[Ir(PCy_3)(COD)(Py)]^+PF_6^-$ are activated in neat pyridine-d_5. Hydride resonances of the complex **1** and **2** are detected after activation (C) and of **2** is removed after addition of $AgPF_6$ to the solution (B). Hydride resonance of **1'** is visible in ^1H NMR spectrum (D) and **2'** manifests itself after addition of DCl (E).

Therefore, we attribute the broad peak at -26.71 ppm in the CEST spectrum (**Figure 1C**) to the exchanging complex **3**, $[Ir(IMes)(Py)_2(CD_3OD)(H)_2]^+Cl^-$**.** In **3**, one of the equatorial positions is occupied by the solvent molecule (CD_3OD). As the peak is broad (FWHM ~4.5 ppm) and no doublet structure is observable, we conclude that **3** is in the intermediate exchange regime between two forms where the solvent occupies one of the two different equatorial positions in the complex. The strong line-broadening of this peak is most likely the reason why it was not detected in previous studies, showing the utility of CEST in detecting such species.

In the following, we discuss the impact of these intermediates on the life-time of the nuclear singlet spin state of hydrogen[26, 28] which is used for the generation of hyperpolarized targets in PHIP and SABRE experiments. The initial spin state of the nuclear spins in parahydrogen is the singlet state which often possesses a significantly longer lifetime compared to standard T_1 relaxation[40-42]:

$$\hat{\rho}_{pH_2} = \frac{\hat{1}}{4} - \left(\hat{I}_{1z}\hat{I}_{2z} + \hat{I}_{1x}\hat{I}_{2x} + \hat{I}_{1y}\hat{I}_{2y}\right).$$

Here $\hat{I}_{1z}\hat{I}_{2z}$ describes the longitudinal and $\hat{I}_{1x}\hat{I}_{2x} + \hat{I}_{1y}\hat{I}_{2y}$ the transversal spin order. Immediately after the parahydrogen addition to the complex, the spins are still in the singlet spin state, however, they start evolving under the nuclear spin Hamiltonian corresponding to the spin system of the complex. In complexes forming typical AX-spin systems with $J_{HH} \ll \Delta\nu$, the transversal components start to oscillate. Combined with the distribution of complexes' formation in time (as is natural for chemical reactions), this causes an efficient decay of the transversal components.[43-45] Furthermore, because the bound hydrogen is in constant exchange with the free hydrogen pool, these complexes provide an efficient pathway of decoherence not only for the bound, but also for the free hydrogen species. The latter can be devastating for SABRE, as the concentration of the SABRE active species responsible for polarization transfer is proportional to the concentration of free parahydrogen, the source of spin order in the hyperpolarization build-up process.[46-47]

Based on this reasoning, we investigated whether it is possible to reduce the amount of singlet-triplet leakage by chemically selecting which intermediates are formed. As the singlet state is not directly observable in NMR experiments, we employed OPSY detection,[48-49] which selectively detects the signal arising from pH_2 in an inequivalent complex such as **2** (**Figure 3A**)). In addition, a spin-locking pulse was applied to further reduce the amount of singlet-triplet leakage by enforcing the same resonance frequency for both dihydride spins of **2** and mitigating weak inequivalencies induced by indirect couplings to other spins.

We applied this scheme to the intermediates **1** and **2**. In complex **1** the dihydride spins have the same chemical shift, which should correspond to weak singlet-triplet leakage. In complex **2**, however, the two hydride spins have a chemical shift difference of 2 ppm, corresponding to $\Delta\nu \approx 1000$ Hz at a field of 11.4 Tesla. This exceeds the typical size of $J_{HH} \approx -8$Hz in these complexes by two orders of magnitude and is thus expected to give rise to significant singlet-triplet leakage.

The relative amounts of **1** and **2** can be chosen by selecting the polarity of the solvent and the counter-ion of the catalytic complex. In the case of a polar, charge-stabilizing solvent like methanol, chlorine readily dissociates from the pre-catalyst and the equilibrium concentration is shifted towards **1**. In case of a non-polar solvent like benzene, the dissociation of chlorine is hindered and **2** is formed preferentially. After eliminating Cl^- from solution (via exchange with the weakly

coordinating PF_6^- ion) **1** becomes the main form again. Accordingly, two samples were prepared in such a way that the chemical equilibrium was shifted strongly to either **1** or **2** (see ESI for details).

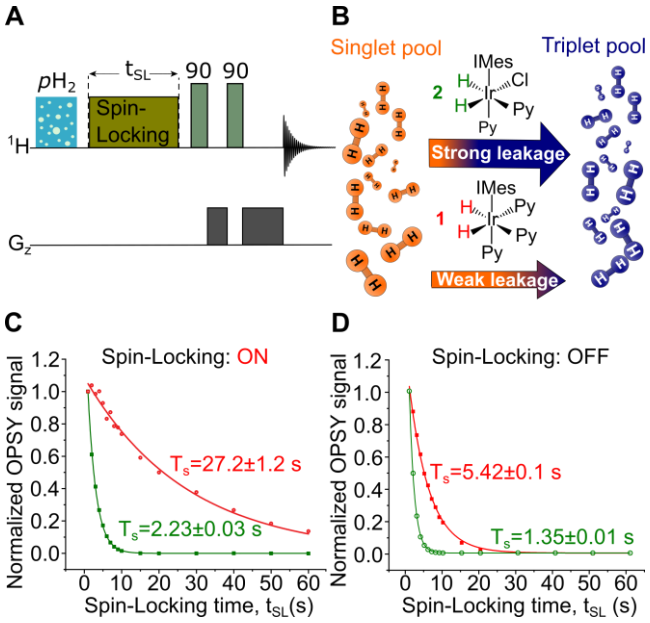

Figure 3: Measurements of the singlet state lifetime of dihydride spins in solution. A) Only-parahydrogen spectroscopy (OPSY) pulse sequence with additional spin-locking pulse (B_1 amplitude 2000Hz, offset frequency -23.1 ppm) was applied after ~30 s of pH_2 bubbling. B) Schematic depiction of the different singlet-triplet leakage pathways. C) Lifetime of non-thermal pH_2-derived spin order in solution of **1** and **2** when spin-locking B_1 field is applied. D) Lifetime of non-thermal pH_2-derived spin order in solution under the same conditions as (C) but without the spin-locking pulse. All measurements were done at 280 K.

Figure 3 compares the singlet life-times of the two samples with and without spin-lock pulse. With the spin locking pulse a lifetime of the pH_2 spin order in solution is 2.23±0.03 s for **2** and of 27.2±1.2 s for **1,** respectively (**Figure 3C**). Without the spin-lock pulse (**Figure 3D**) the lifetimes for **2** and **1** are 1.35±0.03 s and 5.4±0.1 s, respectively. These results clearly corroborate our hypothesis, that it is possible to substantially suppress the singlet-triplet leakage pathway by chemically selecting the proper reaction intermediates.

In conclusion, we have identified a previously non-detectable reversible exchange reaction of chlorine and methanol with Ir-based organometallic catalyst systems used for SABRE hyperpolarization. Furthermore, we show that the chemical-exchange saturation transfer (CEST) scheme is an effective and useful tool to experimentally probe ligand exchange reactions in organometallic complexes. CEST NMR opens the way to gaining experimental insight on reaction dynamics in catalysis and biochemistry (e.g., for studying enzymatic reactions, such as hydrogenase[50]) even in cases where such reactions are inaccessible by conventional or hyperpolarized NMR. We also demonstrate the role of exchanging, low-concentrated intermediate complexes on the spin dynamics of the free pH_2 pool. By removing the complex $[Ir(Cl)(IMes)(H)_2(Py)_2]$ from solution, we show an increase of the singlet state lifetime by more than an order of magnitude, demonstrating a promising new strategy of optimizing SABRE systems for in situ hyperpolarization at high magnetic fields.

ASSOCIATED CONTENT

Supporting Information contains: (i) experimental details and information on the data analysis performed. (ii) additional CEST spectra and fitting details, (iii) SABRE hyperpolarized spectra. (iv) CEST pulse program.

AUTHOR INFORMATION

Corresponding Author

*E-mail: gerd.buntkowsky@chemie.tu-darmstadt.de

Author Contributions

&These authors contributed equally.

ACKNOWLEDGMENTS

Financial support by the Deutsche Forschungsgemeinschaft DFG under contract Bu-911-29-1 and the Russian Science Foundation (grant No. 19-43-04116) is gratefully acknowledged. S.H. thanks the state of Hesse for support in the frame-work of the LOEWE project INAPO.

REFERENCES

1. Dewar, M. J. S.; Talati, A. M., A New Organometallic Semiconductor. *J. Am. Chem. Soc.* **1963,** *85* (12), 1874-1874.
2. Cho, S. J.; Lee, J.; Lee, Y. S.; Kim, D. P., Characterization of Iridium Catalyst for Decomposition of Hydrazine Hydrate for Hydrogen Generation. *Catal. Let.* **2006,** *109* (3), 181-186.
3. Blakemore, J. D.; Schley, N. D.; Balcells, D.; Hull, J. F.; Olack, G. W.; Incarvito, C. D.; Eisenstein, O.; Brudvig, G. W.; Crabtree, R. H., Half-Sandwich Iridium Complexes for Homogeneous Water-Oxidation Catalysis. *J. Am. Chem. Soc.* **2010,** *132* (45), 16017-16029.
4. Climent, M. J.; Corma, A.; Iborra, S., Heterogeneous catalysts for the one-pot synthesis of chemicals and fine chemicals. *Chem. Rev.* **2010,** *111* (2), 1072-1133.
5. Blaser, H.-U.; Malan, C.; Pugin, B.; Spindler, F.; Steiner, H.; Studer, M., Selective Hydrogenation for Fine Chemicals: Recent Trends and New Developments. *Adv. Synth. Catal.* **2003,** *345* (1-2), 103-151.
6. Murahashi, S.-I.; Takaya, H., Low-Valent Ruthenium and Iridium Hydride Complexes as Alternatives to Lewis Acid and Base Catalysts. *Acc. Chem. Res.* **2000,** *33* (4), 225-233.
7. Steigerwald, M. L.; Sprinkle, C. R., Organometallic synthesis of II-VI semiconductors. 1. Formation and decomposition of bis(organotelluro)mercury and bis(organotelluro)cadmium compounds. *J. Am. Chem. Soc.* **1987,** *109* (23), 7200-7201.
8. Klet, R. C.; Kaphan, D. M.; Liu, C.; Yang, C.; Kropf, A. J.; Perras, F. d. r. A.; Pruski, M.; Hock, A. S.; Delferro, M., Evidence for Redox Mechanisms in Organometallic Chemisorption and Reactivity on Sulfated Metal Oxides. *J. Am. Chem. Soc.* **2018,** *140* (20), 6308-6316.
9. Romanenko, I.; Gajan, D.; Sayah, R.; Crozet, D.; Jeanneau, E.; Lucas, C.; Leroux, L.; Veyre, L.; Lesage, A.; Emsley, L., Iridium (I)/N-Heterocyclic Carbene Hybrid Materials: Surface Stabilization of Low-Valent Iridium Species for High Catalytic Hydrogenation Performance. *Angew. Chem. Intl. Ed.* **2015,** *54* (44), 12937-12941.
10. Shin, K.; Park, Y.; Baik, M.-H.; Chang, S., Iridium-catalysed arylation of C–H bonds enabled by oxidatively induced reductive elimination. *Nature Chemistry* **2018,** *10* (2), 218.
11. Hashmi, A. S. K., Homogeneous Gold Catalysis Beyond Assumptions and Proposals—Characterized Intermediates. *Angew. Chem. Intl. Ed.* **2010,** *49* (31), 5232-5241.
12. Pelagatti, P.; Carcelli, M.; Calbiani, F.; Cassi, C.; Elviri, L.; Pelizzi, C.; Rizzotti, U.; Rogolino, D., Transfer Hydrogenation of Acetophenone Catalyzed by Half-Sandwich Ruthenium(II) Complexes Containing Amino Amide Ligands. Detection of the Catalytic Intermediates by Electrospray Ionization Mass Spectrometry. *Organomet.* **2005,** *24* (24), 5836-5844.
13. Bowers, C. R.; Weitekamp, D. P., Para-Hydrogen and Synthesis Allow Dramatically Enhanced Nuclear Alignment. *J. Am. Chem. Soc.* **1987,** *109* (18), 5541-5542.
14. Eisenschmid, T. C.; Kirss, R. U.; Deutsch, P. P.; Hommeltoft, S. I.; Eisenberg, R.; Bargon, J.; Lawler, R. G.; Balch, A. L., Para hydrogen induced polarization in hydrogenation reactions. *J. Am. Chem. Soc.* **1987,** *109* (26), 8089-8091.
15. Green, R. A.; Adams, R. W.; Duckett, S. B.; Mewis, R. E.; Williamson, D. C.; Green, G. G. R., The theory and practice of hyperpolarization in magnetic resonance using parahydrogen. *Prog. Nucl. Magn. Reson. Spectrosc.* **2012,** *67*, 1-48.
16. Pravica, M. G.; Weitekamp, D. P., Net NMR Alignment by Adiabatic Transport of Para-Hydrogen Addition-Products to High Magnetic-Field. *Chem. Phys. Lett.* **1988,** *145* (4), 255-258.
17. Schmidt, A. B.; Berner, S.; Schimpf, W.; Muller, C.; Lickert, T.; Schwaderlapp, N.; Knecht, S.; Skinner, J. G.; Dost, A.; Rovedo, P.; Hennig, J.; von Elverfeldt, D.; Hovener, J. B., Liquid-state carbon-13 hyperpolarization generated in an MRI system for fast imaging. *Nature Comm.* **2017,** *8*.
18. Cowley, M. J.; Adams, R. W.; Atkinson, K. D.; Cockett, M. C. R.; Duckett, S. B.; Green, G. G. R.; Lohman, J. A. B.; Kerssebaum, R.; Kilgour, D.; Mewis, R. E., Iridium N-Heterocyclic Carbene Complexes as Efficient Catalysts for Magnetization Transfer from para-Hydrogen. *J. Am. Chem. Soc.* **2011,** *133* (16), 6134-6137.
19. van Weerdenburg, B. J. A.; Gloggler, S.; Eshuis, N.; Engwerda, A. H. J.; Smits, J. M. M.; de Gelder, R.; Appelt, S.; Wymenga, S. S.; Tessari, M.; Feiters, M. C.; Blumich, B.; Rutjes, F. P. J. T., Ligand effects of NHC-iridium catalysts for signal amplification by reversible exchange (SABRE). *Chem. Comm.* **2013,** *49* (67), 7388-7390.
20. Hovener, J. B.; Bar, S.; Leupold, J.; Jenne, K.; Leibfritz, D.; Hennig, J.; Duckett, S. B.; von Elverfeldt, D., A continuous-flow, high-throughput, high-pressure parahydrogen converter for hyperpolarization in a clinical setting. *NMR in Biomedicine* **2013,** *26* (2), 124-131.
21. Procacci, B.; Roy, S. S.; Norcott, P.; Turner, N.; Duckett, S. B., Unlocking a diazirine long-lived nuclear singlet state via photochemistry: NMR detection and lifetime of an unstabilized diazo-compound. *J. Am. Chem. Soc.* **2018,** *140* (48), 16855-16864.
22. Barskiy, D. A.; Shchepin, R. V.; Coffey, A. M.; Theis, T.; Warren, W. S.; Goodson, B. M.; Chekmenev, E. Y., Over 20% 15N Hyperpolarization in Under One Minute for Metronidazole, an Antibiotic and Hypoxia Probe. *J. Am. Chem. Soc.* **2016,** *138* (26), 8080-8083.
23. Colell, J. F. P.; Logan, A. W. J.; Zhou, Z.; Shchepin, R. V.; Barskiy, D. A.; Ortiz, G. X.; Wang, Q.; Malcolmson, S. J.; Chekmenev, E. Y.; Warren, W. S.; Theis, T., Generalizing, Extending, and Maximizing Nitrogen-15 Hyperpolarization Induced by Parahydrogen in Reversible Exchange. *The Journal of Physical Chemistry C* **2017,** *121* (12), 6626-6634.
24. Rayner, P. J.; Norcott, P.; Appleby, K. M.; Iali, W.; John, R. O.; Hart, S. J.; Whitwood, A. C.; Duckett, S. B., Fine-tuning the efficiency of para- hydrogen-induced hyperpolarization by rational N -heterocyclic carbene design. *Nature Comm.* **2018,** *9* (1), 4251.
25. Zeng, H. F.; Xu, J. D.; Gillen, J.; McMahon, M. T.; Artemov, D.; Tyburn, J. M.; Lohman, J. A. B.; Mewis, R. E.; Atkinson, K. D.; Green, G. G. R.; Duckett, S. B.; van Zijl, P. C. M., Optimization of SABRE for polarization of the tuberculosis drugs pyrazinamide and isoniazid. *J. Magn. Reson.* **2013,** *237*, 73-78.
26. Kiryutin, A. S.; Sauer, G.; Yurkovskaya, A. V.; Limbach, H.-H.; Ivanov, K. L.; Buntkowsky, G., Parahydrogen Allows Ultrasensitive Indirect NMR Detection of Catalytic Hydrogen Complexes. *The Journal of Physical Chemistry C* **2017,** *121* (18), 9879-9888.
27. Knecht, S.; Kiryutin, A. S.; Yurkovskaya, A. V.; Ivanov, K. L., Efficient conversion of anti-phase spin order of protons into 15N magnetisation using SLIC-SABRE. *Mol. Phys.* **2018**, 1-10.
28. Knecht, S.; Kiryutin, A. S.; Yurkovskaya, A. V.; Ivanov, K. L., Mechanism of spontaneous polarization transfer in high-field SABRE experiments. *J. Magn. Reson.* **2018,** *287*, 74-81.
29. Pileio, G.; Hill-Cousins, J. T.; Mitchell, S.; Kuprov, I.; Brown, L. J.; Brown, R. C. D.; Levitt, M. H., Long-Lived Nuclear Singlet Order in Near-Equivalent 13C Spin Pairs. *J. Am. Chem. Soc.* **2012,** *134* (42), 17494-17497.
30. Pravdivtsev, A. N.; Skovpin, I. V.; Svyatova, A. I.; Chukanov, N. V.; Kovtunova, L. M.; Bukhtiyarov, V. I.; Chekmenev, E. Y.; Kovtunov, K. V.; Koptyug, I. V.; Hovener, J. B., Chemical Exchange Reaction Effect on Polarization Transfer Efficiency in SLIC-SABRE. *J. Phys. Chem. A* **2018,** *122* (46), 9107-9114.
31. Theis, T.; Ariyasingha, N. M.; Shchepin, R. V.; Lindale, J. R.; Warren, W. S.; Chekmenev, E. Y., Quasi-Resonance Signal Amplification by Reversible Exchange. *The Journal of Physical Chemistry Letters* **2018,** *9* (20), 6136-6142.
32. Lloyd, L. S.; Asghar, A.; Burns, M. J.; Charlton, A.; Coombes, S.; Cowley, M. J.; Dear, G. J.; Duckett, S. B.; Genov, G. R.; Green, G. G. R.; Highton, L. A. R.; Hooper, A. J. J.; Khan, M.; Khazal, I. G.; Lewis, R. J.; Mewis, R. E.; Roberts, A. D.; Ruddlesden, A. J., Hyperpolarisation through reversible interactions with parahydrogen. *Catal. Sci. Tech.* **2014,** *4* (10), 3544-3554.
33. Guivel-Scharen, V.; Sinnwell, T.; Wolff, S.; Balaban, R., Detection of proton chemical exchange between metabolites and water in biological tissues. *J. Magn. Reson.* **1998,** *133* (1), 36-45.
34. Ward, K.; Aletras, A.; Balaban, R. S., A new class of contrast agents for MRI based on proton chemical exchange dependent saturation transfer (CEST). *J. Magn. Reson.* **2000,** *143* (1), 79-87.
35. Zhou, J.; van Zijl, P. C., Chemical exchange saturation transfer imaging and spectroscopy. *Prog. Nucl. Magn. Reson. Spectrosc.* **2006,** *48* (2-3), 109-136.
36. McMahon, M. T.; Gilad, A. A.; Zhou, J.; Sun, P. Z.; Bulte, J. W. M.; van Zijl, P. C. M., Quantifying exchange rates in chemical exchange saturation transfer agents using the saturation time and saturation power dependencies of the magnetization transfer effect on the magnetic resonance imaging signal (QUEST and QUESP): Ph calibration for poly-L-lysine and a starburst dendrimer. *Magn. Res. Med.* **2006,** *55* (4), 836-847.

37. Lokesh, N.; Seegerer, A.; Hioe, J.; Gschwind, R., Chemical Exchange Saturation Transfer in Chemical Reactions: A Mechanistic Tool for NMR Detection and Characterization of Transient Intermediates. *J. Am. Chem. Soc.* **2018,** *140* (5), 1855-1862.
38. Kiryutin, A. S.; Sauer, G.; Yurkovskaya, A. V.; Limbach, H. H.; Ivanov, K. L.; Buntkowsky, G., Parahydrogen Allows Ultrasensitive Indirect NMR Detection of Catalytic Hydrogen Complexes. *J. Phys. Chem. C* **2017,** *121* (18), 9879-9888.
39. Richards, J. E.; Hooper, A. J. J.; Bayfield, O. W.; Cockett, M. C. R.; Dear, G. J.; Holmes, A. J.; John, R. O.; Mewis, R. E.; Pridmore, N.; Roberts, A. D.; Whitwood, A. C.; Duckett, S. B., Using hyperpolarised NMR and DFT to rationalise the unexpected hydrogenation of quinazoline to 3,4-dihydroquinazoline. *Chem. Comm.* **2018,** *54* (73), 10375-10378.
40. Carravetta, M.; Johannessen, O. G.; Levitt, M. H., Beyond the T-1 limit: Singlet nuclear spin states in low magnetic fields. *Phys. Rev. Lett.* **2004,** *92* (15).
41. Carravetta, M.; Levitt, M. H., Long-Lived Nuclear Spin States in High-Field Solution NMR. *J. Am. Chem. Soc.* **2004,** *126* (20), 6228-6229.
42. Franzoni, M. B.; Buljubasich, L.; Spiess, H. W.; Münnemann, K., Long-Lived 1H Singlet Spin States Originating from Para-Hydrogen in Cs-Symmetric Molecules Stored for Minutes in High Magnetic Fields. *J. Am. Chem. Soc.* **2012,** *134* (25), 10393-10396.
43. Buntkowsky, G.; Bargon, J.; Limbach, H. H., A dynamic model of reaction pathway effects on parahydrogen-induced nuclear spin polarization. *J. Am. Chem. Soc.* **1996,** *118* (36), 8677-8683.
44. Limbach, H. H.; Ulrich, S.; Grundemann, S.; Buntkowsky, G.; Sabo-Etienne, S.; Chaudret, B.; Kubas, G. J.; Eckert, J., NMR and INS line shapes of transition metal hydrides in the presence of coherent and incoherent dihydrogen exchange. *J. Am. Chem. Soc.* **1998,** *120* (31), 7929-7943.
45. Buntkowsky, G.; Limbach, H. H., Dihydrogen Transfer and Symmetry: The Role of Symmetry on the Chemistry of Dihydrogen Transfer in the Light of NMR Spectroscopy. In *Hydrogen-Transfer Reactions*, Hynes, J. P.; Klinman, J. P.; Limbach, H. H.; Schowen, R. L., Eds. Wiley-VCH: Weinheim, 2006; Vol. 2 pp 639-682.
46. Knecht, S.; Pravdivtsev, A. N.; Hövener, J.-B.; Yurkovskaya, A. V.; Ivanov, K. L., Quantitative description of the SABRE process: rigorous consideration of spin dynamics and chemical exchange. *RSC Advances* **2016,** *6* (29), 24470-24477.
47. Barskiy, D. A.; Pravdivtsev, A. N.; Ivanov, K. L.; Kovtunov, K. V.; Koptyug, I. V. J. P. C. C. P., A simple analytical model for signal amplification by reversible exchange (SABRE) process. **2016,** *18* (1), 89-93.
48. Aguilar, J. A.; Elliott, P. I. P.; López-Serrano, J.; Adams, R. W.; Duckett, S. B., Only para-hydrogen spectroscopy (OPSY), a technique for the selective observation of para-hydrogen enhanced NMR signals. *Chem. Comm.* **2007,** *0* (11), 1183-1185.
49. Savka, R.; Plenio, H., Facile synthesis of [(NHC)MX(cod)] and [(NHC)MCl(CO) 2] (M = Rh, Ir; X = Cl, I) complexes. *Dalton T.* **2015,** *44* (3), 891-893.
50. Rumpel, S.; Sommer, C.; Reijerse, E.; Farès, C.; Lubitz, W., Direct Detection of the Terminal Hydride Intermediate in [FeFe] Hydrogenase by NMR Spectroscopy. *J. Am. Chem. Soc.* **2018,** *140* (11), 3863-3866.

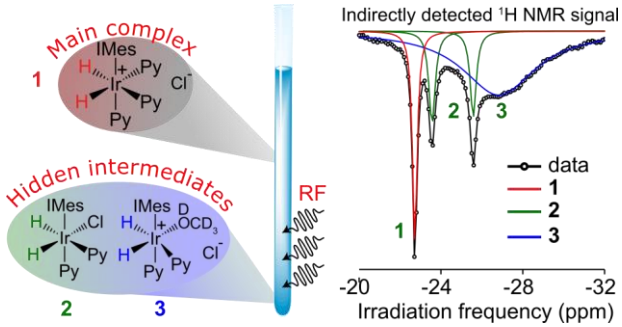
Main complex
1
IMes
Py
Cl
Py
Py
Hidden intermediates
IMes
Cl
Py
Py
IMes
D
OCD3
Cl
Py
Py
2
3
RF
Indirectly detected ¹H NMR signal
1
2
3
data
1
2
3
-20
-24
-28
-32
Irradiation frequency (ppm)

TOC graphic

Electronic Supporting Information

Indirect Detection of Short-lived Hydride Intermediates of Iridium N-Heterocyclic Carbene Complexes via Chemical Exchange Saturation Transfer (CEST) Spectroscopy

Stephan Knecht[a,b&], Sara Hadjiali,[a&], Danila A. Barskiy[c&], Alexander Pines[c], Grit Sauer[a], Alexey S. Kiryutin[d], Konstantin L. Ivanov[d], Alexandra V. Yurkovskaya[d] and Gerd Buntkowsky[a*]

[a]*Eduard-Zintl Institute for Inorganic and Physical Chemistry, TU Darmstadt, Darmstadt, 64287, Germany*
[b] *Department of Radiology, Medical Center – University of Freiburg, Freiburg, 79106, Germany*
[c]*Department of Chemistry, University of California at Berkeley, CA 94720-3220*
[e] *International Tomography Center, Siberian Branch of the Russian Academy of Science, Novosibirsk, 630090, Russia and Novosibirsk State University, Novosibirsk, 630090, Russia*

Experimental Methods

Sample Preparation

The pre-catalysts were dissolved in the deuterated solvent (pyridine-d_5, methanol-d_4, benzene-d_6) and the substrate was added. To exchange the Cl^- with the PF_6^- ion, $AgPF_6$ was added in an equimolar amount to the catalyst, leading to AgCl (if it formed). Subsequently, the AgCl was removed from the sample by centrifugation. When pyridine-d_5 was used as the solvent, the $AgPF_6$ salt was added after activation. In methanol and benzene, the salt was added prior to the activation of the pre-catalyst. All samples were activated either by bubbling H_2 under 3 atm pressure or in a pressure tube using 9 atm of H_2. All substrates and solvents were purchased from Sigma-Aldrich. Pre-catalyst [Ir(IMes)(COD)(Cl)] (**1***) was synthesized as previously reported[1]. Crabtree's catalyst was purchased from Strem Chemicals. All chemicals were used as received without further purification.

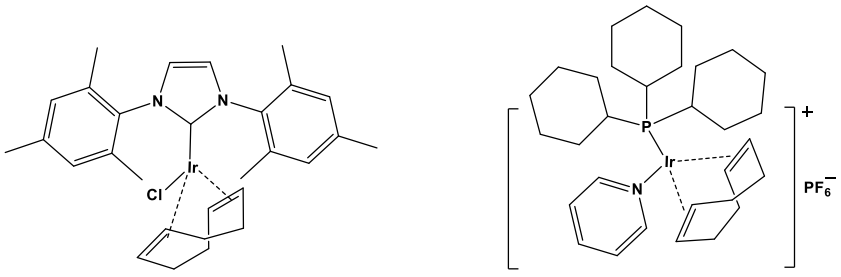

1* Crabtree´s catalyst

Scheme S1: Structures of the pre-catalysts used in this work. Left: [Ir(IMes)(COD)(Cl)] (**1***), right: [Ir(Py)(PCy_3)(COD)] PF_6^- (Crabtree's catalyst)

Detailed preparation steps:

1. Preparation of **1** $[Ir(IMes)(H)_2(Py)]^+Cl^-$, **2** $[Ir(IMes)(Cl)(H)_2(Py)_2]$ and **3** $[Ir(IMes)(CD_3OD)(H)_2(Py)_2]$ in methanol-d_4:
   Pre-catalyst [IrCl(IMes)(COD)] (2.25 mM) was dissolved in 600 µL of methanol-d_4 and 13.8 mM of pyridine was added, yielding a light yellow. The solution was bubbled with hydrogen at 3 bar pressure until it turned transparent and full conversion of the pre-catalyst was confirmed by PASADENA measurements as described before. The presence of **1**, **2** and **3** is confirmed by the data presented in the main text.

2. Preparation of **1** $[Ir(IMes)(H)_2(Py)_3]^+PF_6^-$, **2** $[Ir(IMes)(H)_2(CD_3OD)(Py)_2]^+PF_6^-$ in methanol-d_4:
   Pre-catalyst [IrCl(IMes)(COD)] (2.25 mM) was dissolved in 600 µL of methanol-d_4 and 13.8 mM of pyridine was added, yielding a light yellow liquid. An equimolar amount of $AgPF_6$ (2.25 mM) was added. Within seconds, a white salt (AgCl) precipitated and was removed from solution via centrifugation. The solution was bubbled with hydrogen at 3 bar pressure until it turned transparent and full conversion of the pre-catalyst was confirmed by PASADENA measurements[2].

3. Preparation of **2** $[Ir(Cl)(H)_2(Py)_2]$ in benzene-d_6:
   Pre-catalyst [IrCl(IMes)(COD)] (4.3 mM) was dissolved in 700 µL of benzene-d_6 and 70 mM of pyridine was added, yielding a light to dark yellow liquid. The solution was bubbled with hydrogen at 3 bar pressure until it turned to a light yellow, almost transparent Liquid. Full conversion of the pre-catalyst was confirmed by PASADENA measurements as described before[2] The presence of **2** was confirmed by NMR, also traces of **1** were detected by NMR, the ratio of **1**:**2** was 1:40 at 280K sample temperature

4. Preparation of **1** $[Ir(IMes)(H)_2(Py)_3]^+PF_6^-$, in benzene-$d_6$:
   Pre-catalyst [IrCl(IMes)(COD)] (4.3 mM) was dissolved in 700 µL of *d* benzene-d_6 and pyridine solution of $AgPF_6$ was added resulting in the final concentrations of 70 mM and 5 mM for pyridine and $AgPF_6$ respectively. Within seconds white (AgCl) and yellow ($AgPF_6$) salts participated and were removed by centrifugation. The solution was bubbled with hydrogen at 3 bar pressure until it turned transparent and full conversion of the pre-catalyst was confirmed by PASADENA measurements[2]. Presence of **1** was confirmed by NMR and traces of **2** were detected by PASADENA hyperpolarized NMR.

5. Preparation of **1** $[Ir(IMes)(H)_2(Py)_3]Cl$, **2** $[Ir(Cl)(H)_2(Py)_2]$ in pyridine-d_5:
   Pre-catalyst [IrCl(IMes)(COD)] (11 mM) was dissolved in 600 µL of pyridine-d_5, yielding a light to dark yellow solution. The solution was exposed to hydrogen in a pressure tube at 10 bar for 2 hours, until it turned into a light yellow liquid. The presence of **1** and **2** was confirmed by NMR.

6. Preparation of **1** $[Ir(IMes)(H)_2(Py)_3]Cl$ in pyridine-d_5:
   A solution was prepared according to 5. Afterwards, an equimolar amount of $AgPF_6$ (11 mM) was added to the solution. NMR measurements confirmed the disappearance of **2** from the sample

7. Preparation of **1** [Ir(PCy$_3$)(H)$_2$(Py)$_3$]PF$_6^-$, in pyridine-d$_5$:
   Pre-catalyst [Ir(Py)(PCy$_3$)(COD)] (11 mM) was dissolved in 600 µL of pyridine-d$_5$, yielding a light to dark yellow solution. The solution was exposed to hydrogen in a pressure tube at 10 bar for 2 hours, until it turned into a light yellow liquid. The presence of 1 was confirmed by NMR.
8. Preparation of **2** [Ir(Cl)(PCy$_3$)(H)$_2$(Py)$_2$]$^+$PF$_6^-$ in pyridine-d$_5$:
   A solution was prepared according to 7 and 20 µL of a 38 % concentrated DCl solution was added. The appearance of **2** was confirmed by NMR (see the main text).

NMR methods

CEST experiments

The CEST experiments were conducted according to the pulse sequence shown in Scheme 1 of the main text. The signal of the observed lines was normalized to yield the CEST spectra reported:

$$S_{CEST} = \frac{S_{RF}}{S_0} - 1,$$

where S_{RF} is the intensity under CW-saturation and S_0 is the NMR line intensity without irradiation. In all CEST experiments reported, the intensity of the free H_2 line was measured and no hyperpolarization was used for the CEST measurements. The following Lorentz function, describing the individual peaks, was used for fitting:

$$y = \frac{2A}{\pi}\frac{\omega}{4(x - x_c)^2 + \omega^2}.$$

The obtained parameters are given in Table ST1 and fits are plotted in the Figure 2 of the main text.

Table ST1: Parameters from Lorentzian line fitting of the complexes:

Complex	x_c(ppm) - position	ω(ppm) -FWHM	A (ppm) - area
1	-22.72 ± 0.01	0.29 ± 0.01	-0.46 ± 0.01
2	-25.58 ± 0.01 (H_b) -23.56 ± 0.01 (H_a)	0.36 ± 0.02	-0.11 ± 0.01
3	-26.71 ± 0.11	4.78 ± 0.5	-0.71 ± 0.07

Hyperpolarized NMR experiments

Hyperpolarized experiments were performed either directly at high field NMR spectrometer (proton Larmor frequency 500 MHz) or in the stray field of the magnet at a field at ~ 5 mT. Parahydrogen (pH_2) enrichment was 50 % in all experiments. Bubbling was performed under 3 atm of pressure using a previously described homemade setup[3].

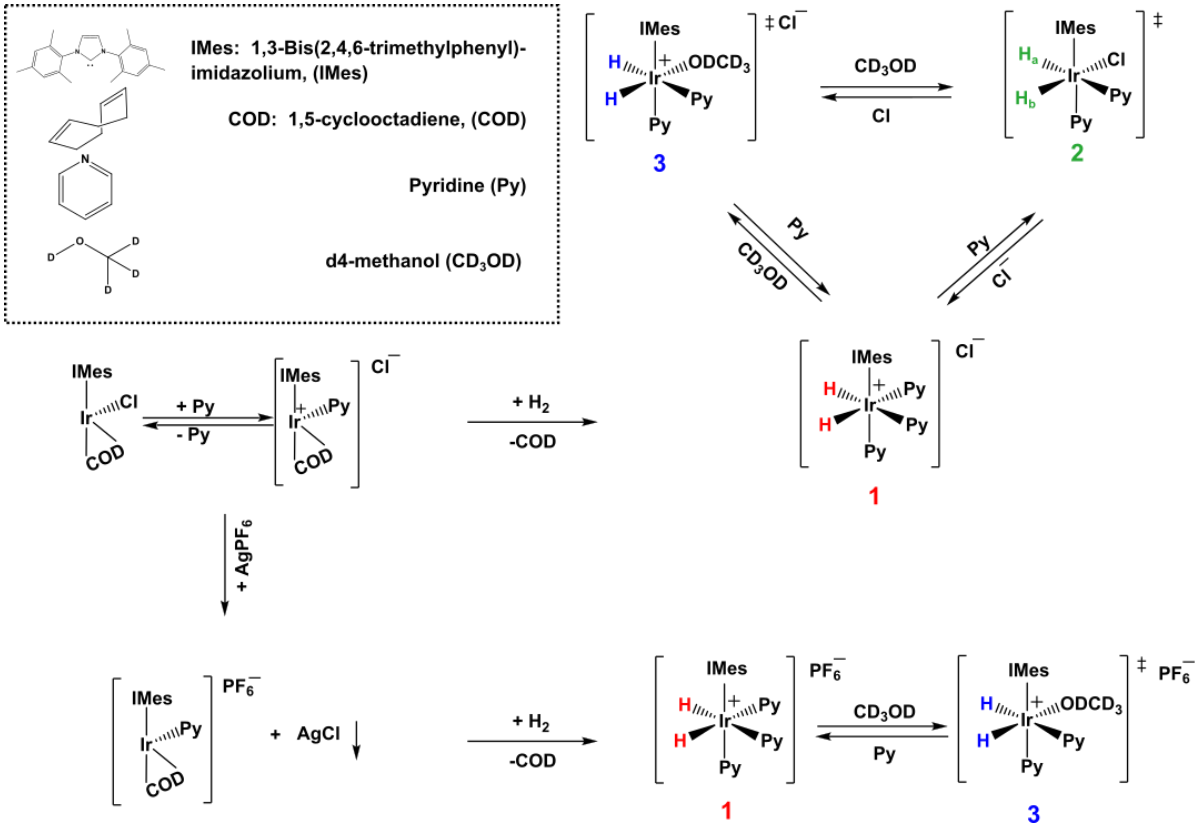

Scheme S2: Activation pathway of the pre-catalyst and intermediates present in the system without (top) and with the addition of $AgPF_6$ (bottom). Assignment of the protons of **2** was done by low-temperature (260 K) PASADENA measurements in methanol-d_4. The chemical shifts of **1**,**2** and **3** can be found in table ST1

Additional CEST spectra

CEST spectra of **1** in methanol-d_4 before and after ion exchange from Cl^- to PF_6 are reported in figure S1. Note the disappearance of the hydrides of **2** when chlorine is removed from the sample.

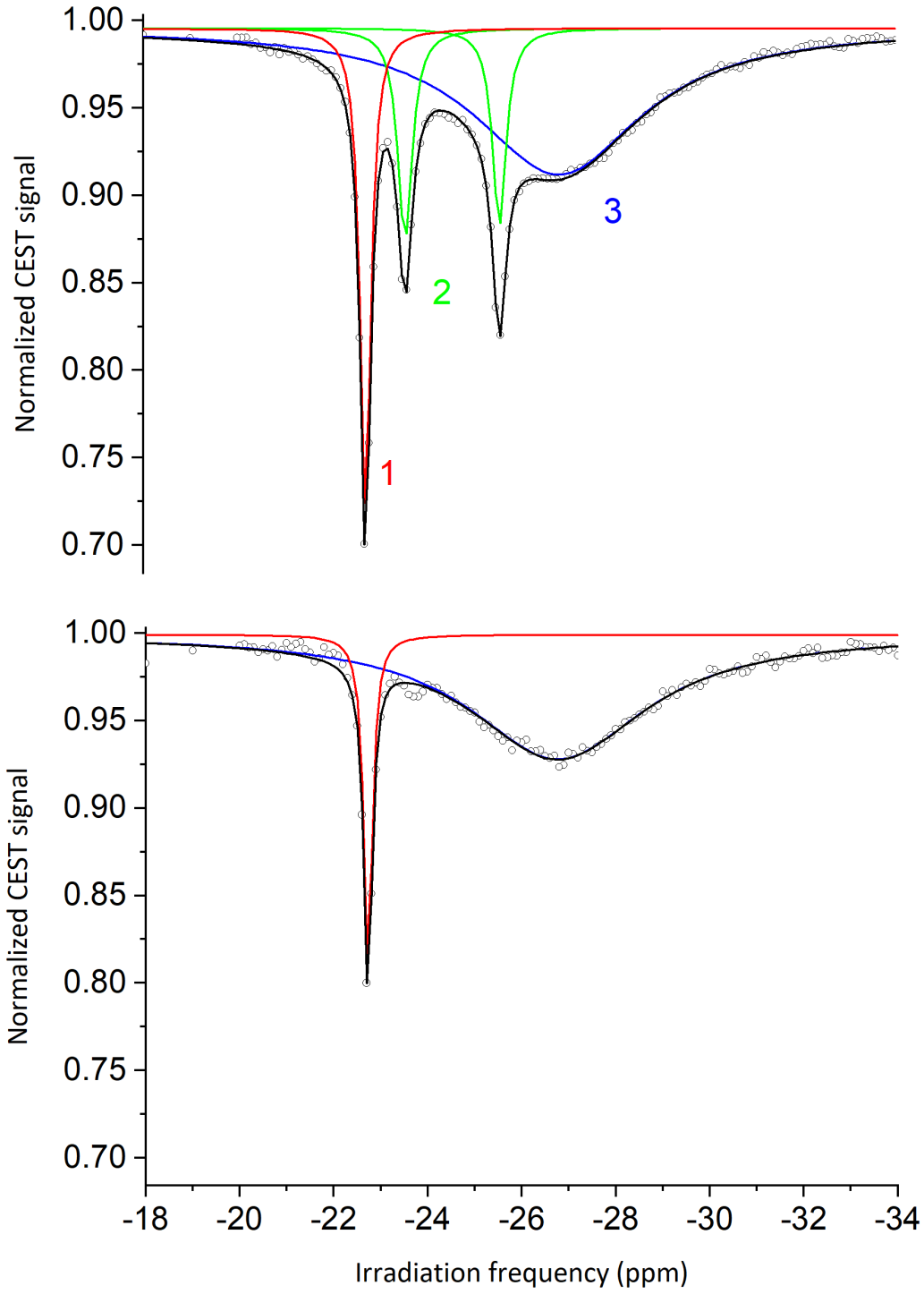

Figure S1: Top: ^{1}H NMR CEST spectrum of **1** in methanol at 280 K showing the presence of dihydride intermediates **2** and **3**. Bottom: CEST measurements, after addition of $AgPF_6$ and removal of AgCl from the sample, note that the CEST peaks corresponding to hydride peaks of **2** are significantly reduced. Grey squares and line — experimental data; red, blue and green lines are Lorentzian fits.

The same CEST measurement as reported in the main text was carried out at room temperature (298 K). The data in Figure S1 shows the same lines as are reported in the main text, albeit that there are more difficult to distinguish because of their overlap. Note that the magnitude of the CEST effect is stronger at room temperature because of the faster ligand exchange

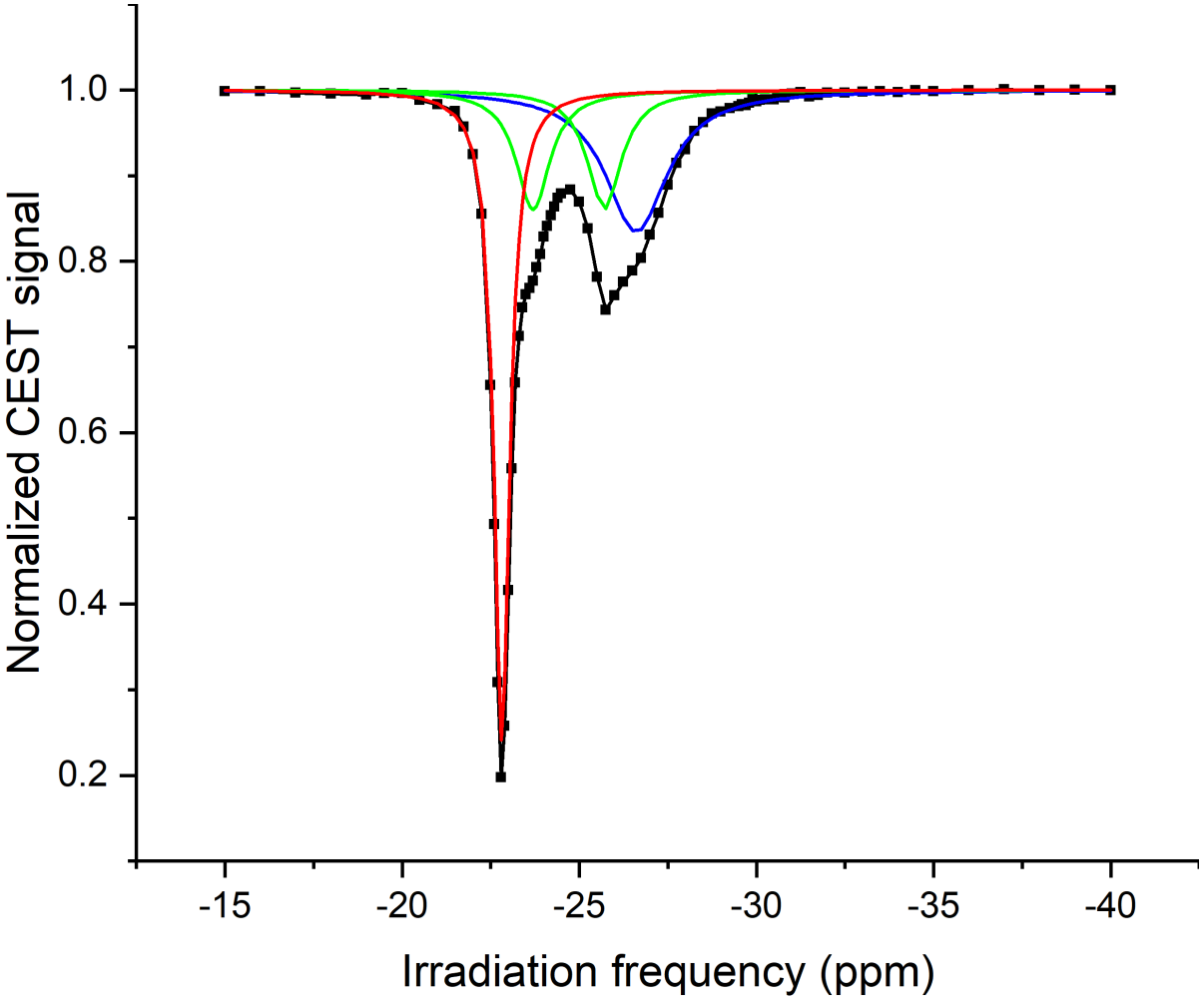

Figure S2: ^{1}H NMR CEST spectrum in methanol-d_4 recorded under the same conditions as the data reported in Figure 1 of the main text, but at room temperature (298 K). The data shows, that the intermediates 1 and 2 can also be distinguished at room temperature. Grey squares and line — experimental data; red, blue and green lines are Lorentzian fits.

Additionally, we present a CEST measurement of the same sample, when the free hydrogen pool has been removed from solution by several minutes of helium bubbling (Figure S3). In this case, the line intensity of the main species is plotted. The resulting CEST spectra clearly shows, that these complexes undergo interexchange (via substrate ligand exchange, compare scheme in figure 1 in the main text), even in the absence of a free hydrogen pool.

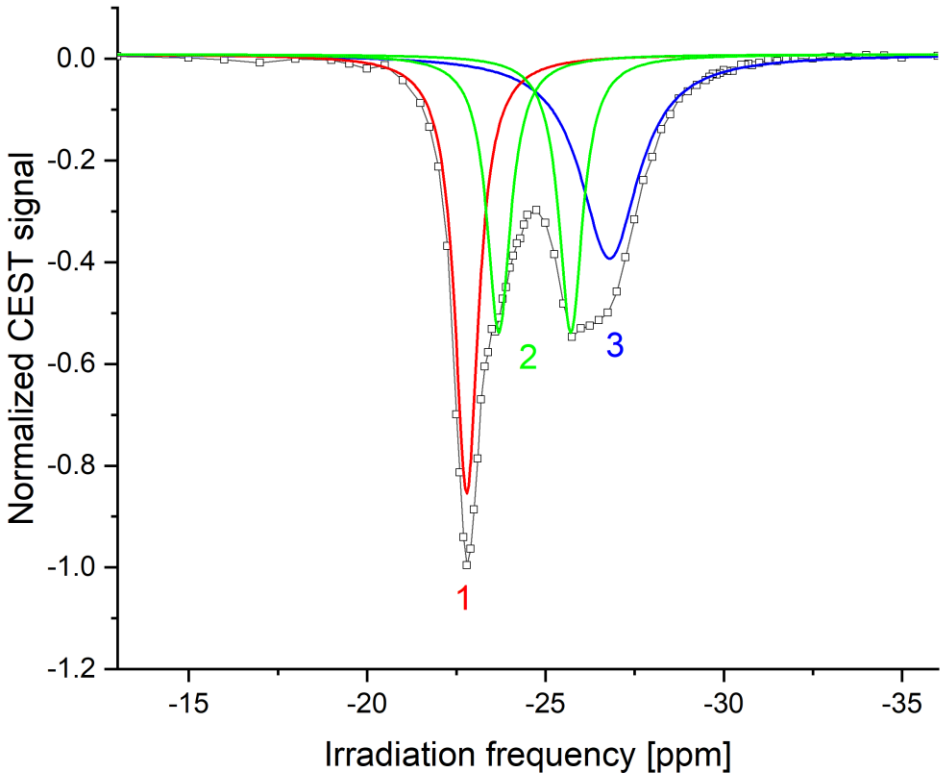

Figure S3: ^{1}H NMR CEST spectrum of **1** in methanol at 298K, after the free hydrogen pool was removed via helium bubbling, showing the presence of dihydride intermediates **2** and **3**. Grey squares and line — experimental data; red, blue and green lines are Lorentzian fits.

Hyperpolarized NMR spectra

SABRE hyperpolarization experiments were conducted before and after ion exchange of chlorine to PF_6^- in methanol and benzene. The SABRE enhancements are comparable, or even better when PF_6^- is the counterion of the SABRE active catalyst.

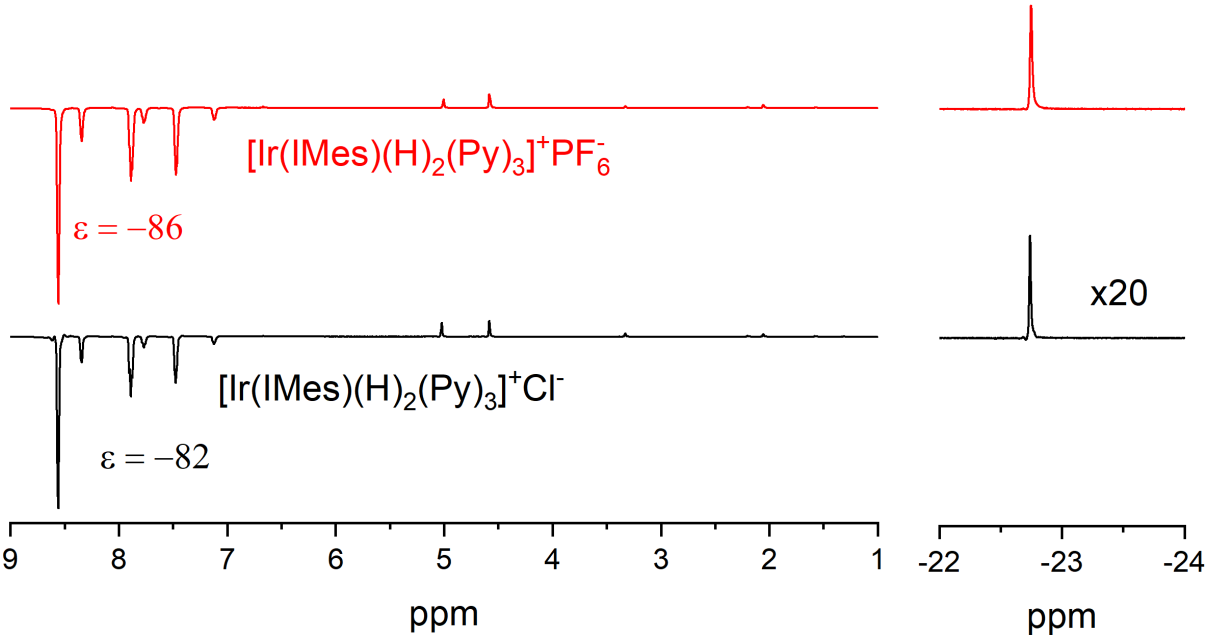

Figure S4: SABRE enhanced spectra of pyridine in methanol-d_4, with PF_6^- (top) or chloride (bottom) used as counter ion. The sample was polarized in the stray field of a 500 MHz NMR at ~5 mT.

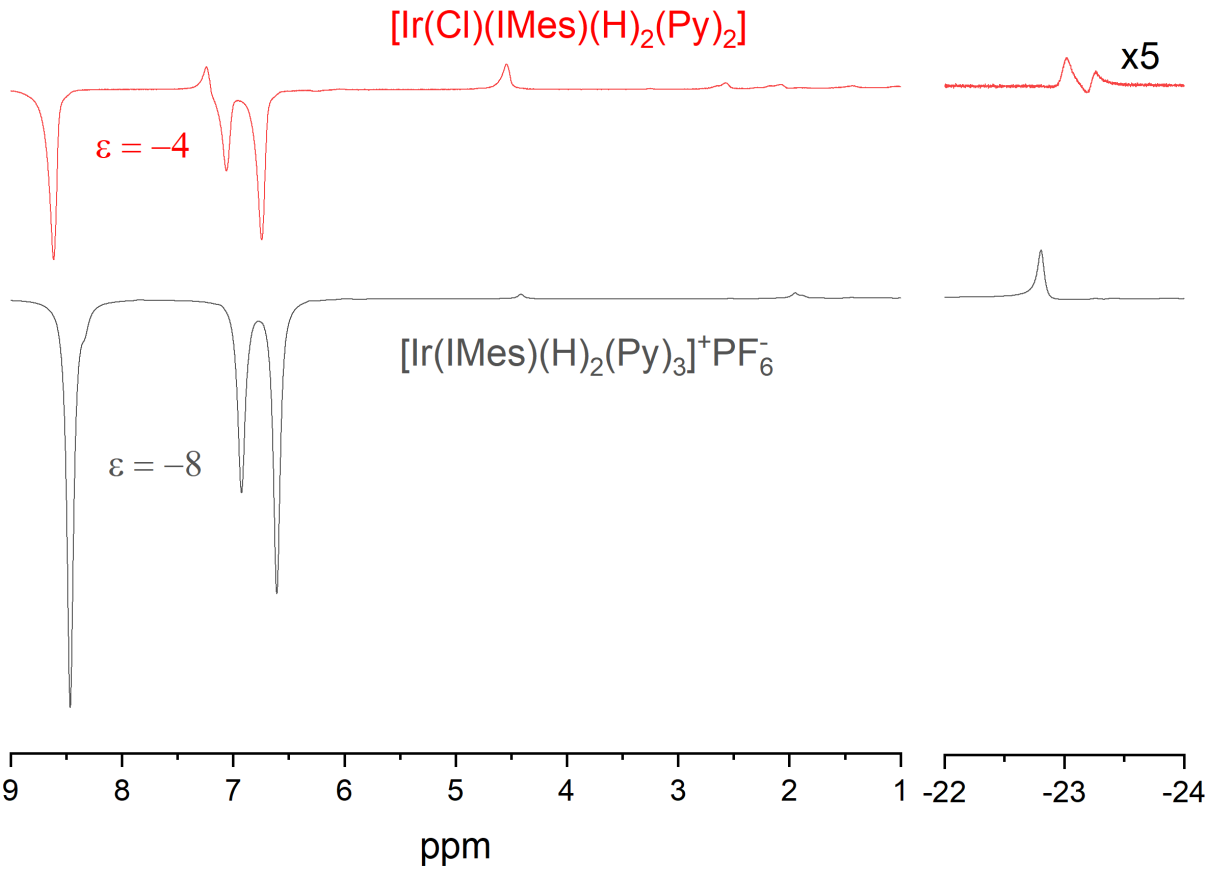

151

152

153 **Figure S5:** Low-field SABRE enhanced spectra of pyridine in benzene-d_6, with the counter ion Cl^-
154 (top) and PF_6^-(bottom). The sample was polarized in the stray field of a 500 MHz NMR at ~5 mT.

155

Lifetime measurements of the singlet-state.

For the determinisation of the lifetimes of the singlet state in the complexes[Ir(IMes)$(H)_2(Py)_3]^+PF_6^-$ (**1**) and [Ir(Cl)(IMes)$(H)_2(Py)_2$] (**2**) two different samples were prepared according to the description provided above, where one of the forms is the dominant one. Figure S6 shows a spectrum of a solution of benzene, where **1** is the dominant form. The hydrides of species **2** are only visible in hyperpolarized spectra. For the determination of the singlet state lifetime, OPSY measurements with and without spin-locking of the hydrides were performed as described in the main text. The signal evaluated for the lifetime measurements was the hyperpolarized species of the hydrides of **2** as the chemically equivalent hydrides of **1** are not visible when the OPSY coherence filter is applied.

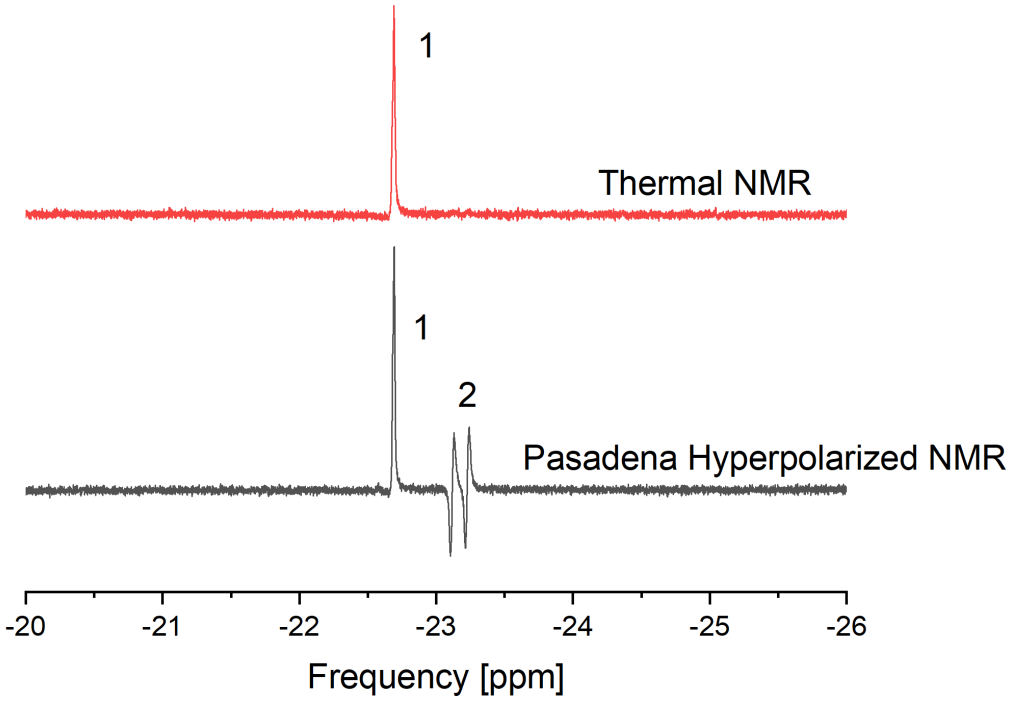

Figure S6: Top: Thermally polarized NMR spectrum of **1** [Ir(IMes)$(H)_2(Py)_3]PF_6$ in benzene-d_6. Bottom: PASADENA-polarized spectrum of the same sample. Note that the low concentrated species of **2** [IrCl(IMes)$(H)_2(Py)_2$] is now visible as antiphase peaks. The amplitude of this species was evaluated in the lifetime measurements presented in Figure 3 of the main text.

Experimental optimization and exchange rates

The duration of the saturation pulse in the ^{1}H NMR CEST approach needs to be optimized experimentally. Moreover, the dependence of CEST signal intensity on the saturation pulse length can be used to obtain an approximate values of the hydrogen exchange rates active in the system under investigation. Figure S7 shows the CEST reduction of the free H_2 line intensity (normalized to the value without irradiation) for irradiation applied on the resonances of complexes **1** (-22.7 ppm), **2** (-23.5 or -25.5 ppm), and **3** (-27ppm) at a temperature of 280 K. For the spectra reported in the main text we choose a duration of 3 seconds for time efficiency (relative saturation value is 85-95%). In order to obtain an approximated values of the exchange rates in the system, we used a simple two-site exchange model. In this case, the evolution of the magnetization of the free H_2 pool can be described by a simple differential equation:

$$\frac{d}{dt}M_z(t) = -\left(R_1 + k^a_{\mathrm{H}_2}\right)M_z(t) + M_z^{eq}R_1 + k^d_{\mathrm{H}_2}M_z^C(t). \quad \text{S1}$$

Where R_1 is the longitudinal relaxation rate, $k^a_{\mathrm{H}_2}$ is the rate of hydrogen association to the complex, $k^d_{H2}$is the dissociation rate of H_2 from the complex, $M_z^C(t)$ is the magnetization of complex bound H_2 and M_z^{eq} is the equilibrium magnetization of free H_2without saturation. For simplicity, we assume that hydrogen bound to the complex is immediately saturated upon application of the saturation pulse, meaning $M_z^C(t) = 0$ at all times. Under these conditions, the equation S1 is readily solved and yields a simple exponential dependence:

$$M_z(t) = \frac{R_1 M_z^{eq}}{R_1 + k^a_{\mathrm{H}_2}} + \left(M_z^{eq} - \frac{R_1 M_z^{eq}}{R_1 + k^a_{\mathrm{H}_2}}\right)e^{-\left(R_1 + k^a_{\mathrm{H}_2}\right)t}. \quad \text{S2}$$

When the concentration of both exchanging species is known (as is the case for Complex **1**), association and dissociation rates can be approximated using the equilibrium condition $k^a_{\mathrm{H}_2}[\mathrm{H}_2] = k^d_{\mathrm{H}_2}[\mathrm{C}]$, where [C] is the concentration of the complex in question. We report both these rates for complex **1** at 280 K and 300 K in Table S1. It is noteworthy, that the dissociation at 300 K is in good agreement to that expected from literature [4] of 20 s^{-1}. For complexes **2** and **3** we give $k^d_{H2}[\mathrm{H}_2]$ as a useful measure for the amount of H_2 being exchanged by these complexes (the hydrogen concentration in our experiments was 16 mM. It should be noted, that with the 50 Hz amplitude used in our studies, only one resonance of complex 2 can be excited (thus the obtained value from the fit needs to be multiplied by 2). It should be noted, that the uncertainties in the table were obtained by fitting equation S2 to the data shown in figure S7 and do not take into account systematic errors induced by the simplification of this approach.

Table S1: Association and dissociation rates of the main SABRE complex **1.**

Temperature (K)	$k^d_{\mathrm{H}_2}$ (s^{-1})	$k^a_{\mathrm{H}_2}$ (s^{-1})
300	15.8±0.1	2.82±0.01
280	1.57±0.1	0.28±0.01

Table S2: Association rates of the SABRE complexes **2** and **3** at 280 K

Complex	$k_{H2}^{a}(s^{-1})$	$k_{H2}^{a}[H_2]\ (s^{-1}mM)$
2	0.24±0.02	3.84±0.32
3	0.06±0.01	0.96±0.16

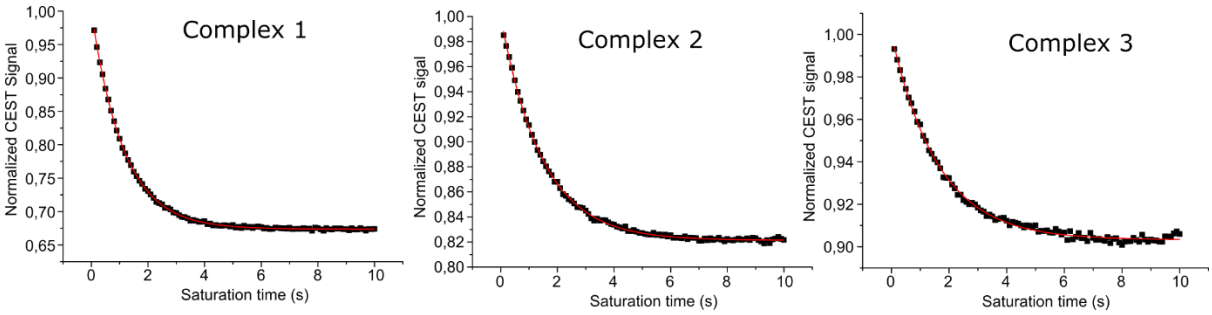

Figure S7. Dependence of the normalized CEST signal on the saturation time (saturation pulse was applied in resonance with hydride NMR lines of the complexes **1**, **2**, and **3**, respectively).

Pulse Program

The following pulse program implements the CEST experiment on a Bruker Avance III running TopSpin 3.2. The use of frequency lists is described in the TopSpin pulse programming manual. The purge gradient reduces artefacts and distortions resulting from coherences (transversal magnetization) excited during the CW-saturation and can be omitted if necessary.

```
;CEST experiment with purge gradient
;$CLASS=HighRes
;$DIM=2D
;$TYPE=
;$SUBTYPE=
;$COMMENT=
;$RECOMMEND=y


#include <Avance.incl>
"acqt0=-p1*2/3.1416"

define list<frequency> fqlist=<$FQ1LIST>

1 ze
 10u fqlist:f2
 20u fqlist.inc

2 d1
   d2 cw:f2  ; wait during saturation delay
```

```
  20u do:f2 ; turn off saturation
  d22 gron1 ; apply purge gradient for time d22
  d23 groff ; turn off gradient and allow for recovery during d23
  p1 ph1
  go=2 ph31
  50m wr #0 if #0

  lo to 1 times td1

exit


ph1=0
ph31=0


;pl1 : f1 channel - power level for pulse (default)
;pl2: f2 channel -  power for CW saturation
;p1 : f1 channel -  90 degree high power pulse
;d1 : T1 recovery time
;d2 : time of CW saturation
;d22: purge gradient time ((purge gradients are often not necessary)
;d23: gradient recovery time
;td1: number of experiments = number of elements in frequency list 1
;ns: 1*n

;Written by Stephan Knecht (knecht@chemie.tu-darmstadt.de).
```

References

1. Savka, R.; Plenio, H., Facile synthesis of [(NHC)MX(cod)] and [(NHC)MCl(CO)2] (M = Rh, Ir; X = Cl, I) complexes. *Dalton Trans* **2015,** *44* (3), 891-3.
2. Truong, M. L.; Shi, F.; He, P.; Yuan, B.; Plunkett, K. N.; Coffey, A. M.; Shchepin, R. V.; Barskiy, D. A.; Kovtunov, K. V.; Koptyug, I. V.; Waddell, K. W.; Goodson, B. M.; Chekmenev, E. Y., Irreversible Catalyst Activation Enables Hyperpolarization and Water Solubility for NMR Signal Amplification by Reversible Exchange. *J. Phys. Chem. B* **2014,** *118* (48), 13882-13889.
3. Kiryutin, A. S.; Sauer, G.; Hadjiali, S.; Yurkovskaya, A. V.; Breitzke, H.; Buntkowsky, G., A highly versatile automatized setup for quantitative measurements of PHIP enhancements. *J Magn Reson* **2017,** *285*, 26-36.
4. Cowley, M. J.; Adams, R. W.; Atkinson, K. D.; Cockett, M. C. R.; Duckett, S. B.; Green, G. G. R.; Lohman, J. A. B.; Kerssebaum, R.; Kilgour, D.; Mewis, R. E., Iridium N-Heterocyclic Carbene Complexes as Efficient Catalysts for Magnetization Transfer from para-Hydrogen. *J. Am. Chem. Soc.* **2011,** *133* (16), 6134-6137.